

## Abstract

A huge part of Earth's life develops in coastal areas, therefore, these zones are of paramount importance to humans for several aspects, both civil and scientific. Many coastal physical phenomena are strictly dependent on winds, such as currents, the diffusion of pollutants, heat, momentum, nutrients etc, therefore, their accurate estimate at high spatial resolutions is fundamental. Coastal winds derived from scatterometers may be affected by biases caused by normalized radar cross section ( $\sigma_0$ ) contamination from land [1], implying that current scatterometer-derived winds may be flagged within  $\approx 25$  km to the coastline. To overcome this issue, several empirical  $\sigma_0$  correction methods have been developed in the recent past [2,3], but some scientific questions about the accuracy of the retrieved winds are still open. This study presents the application of the "noise-regularization" procedure to the QuikSCAT  $\sigma_0$ s to improve both sampling and accuracy of the retrieved winds along the coasts. In this study, three retrieval experiments are shown to assess the improvement of coastal sampling and the impact of land mitigation on the retrieved winds. The results show that the coastal sampling improves by a factor 4 within 5 km and by a factor  $\approx 3$  within 10 km from the coastline. Their comparison to collocated ECMWF winds show that biases increase towards the coast, but nothing can be said about their source, whether it is due to the model or any residual land contamination. The distributions of the retrieved winds suggest that  $\sigma_0$ s within 10 km could be under corrected, but this aspect deserves further investigations.

## Dataset

- 10<sup>th</sup> April 2007 (14 orbits)
- Quality Control:
  - No issues in the communication
  - Good telemetry
  - No requirements on  $sgn(\sigma_0)$ , SNR and the range of values of  $\sigma_0$

## Methodology

- Computation of Land Contribution Ratio ( $f$ ) [1]
- $\sigma_0$  correction.
  - Hypothesis:
    - Linear dependency of  $\sigma_0$  on  $f$ :  $\sigma_0 = af + b + \epsilon$
    - $\sigma_0^{LAND}$  and  $\sigma_0^{SEA}$  are locally homogeneous
  - Regression of  $a$  and  $b$  on a 5x5 Wind Vector Cell (WVC) grid of 12.5 km [2]
  - $\bar{\sigma}_0 = af + b$  represents the expected value of  $\sigma_0(f)$
  - $\bar{\sigma}_0(f)$  is used to query a LUT of pre-computed  $K_p$ s, as described in [4]
  - $\sigma_0$  is distributed as:  $\chi^2_{Norm}(\bar{\sigma}_0, K_p)$
  - $K_p$  is the specific  $\sigma_0$  noise
- Noise regularization is applied to contaminated  $\sigma_0$ s with  $f > 0.5$ . (see Fig. 1)

$$f = \frac{\sum_{xy} S_{xy} L_{xy}}{\sum_{xy} S_{xy}}$$

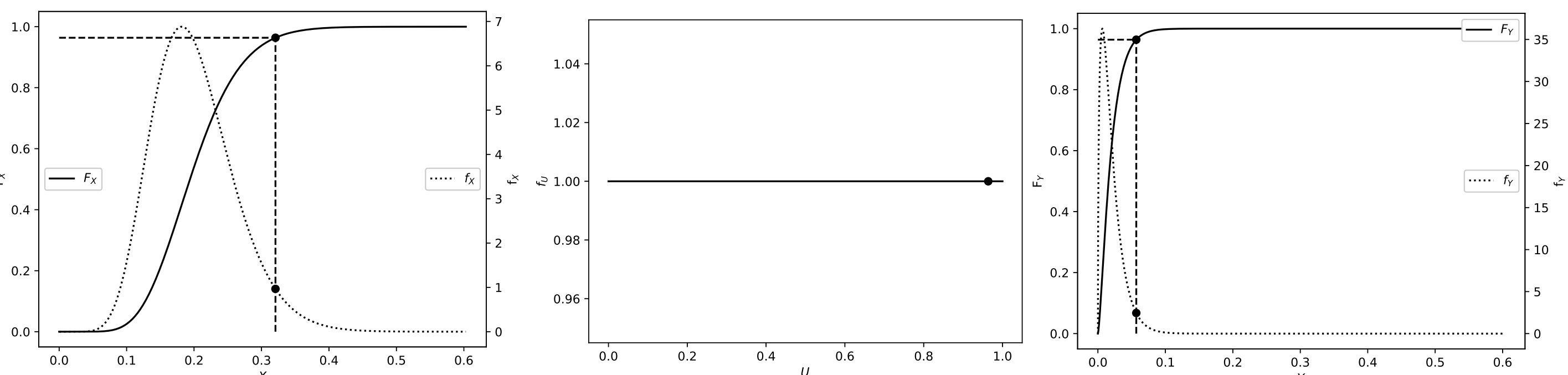


Fig. 1: Graphical demonstration of how noise regularization works. Left plot: dotted (solid) line represents the pdf (CDF) of the contaminated  $\sigma_0$ s. The black circle represents one realization of the contaminated  $\sigma_0$ s ( $X$ ). The value of  $F_x(X)$  is made with the same black circle in the central plot ( $f_x(U)$ ), which represents an homogeneous pdf. In fact,  $F_x$  values (and so do  $F_y$ ) are distributed as a homogeneous pdf between 0 and 1. Right plot: dotted (solid) line represents the pdf (CDF) of the non-contaminated  $\sigma_0$ s. The black circle represents the projection of  $X$  on the domain of the non-contaminated  $\sigma_0$ s ( $Y$ ).

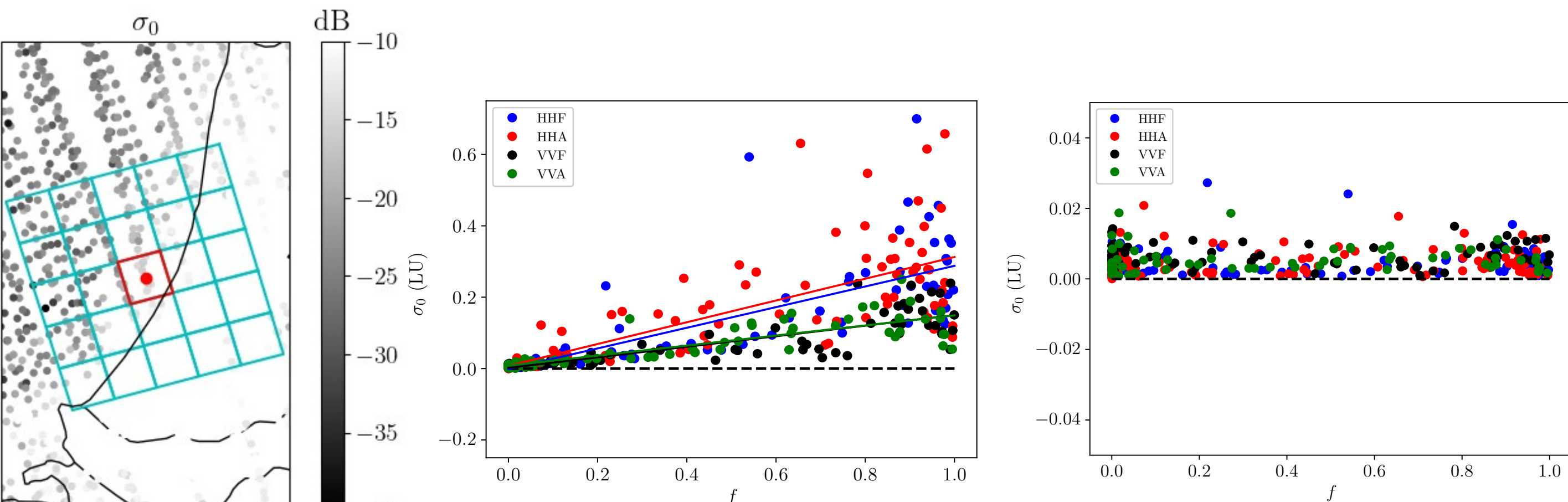


Fig. 2:  $\sigma_0$ s in dB offshore Netherlands. Cyan boxes: WVCs at 12.5 km used for regression when corrections are applied to slices in the red framed WVC. Fig. 3: Scatter-plot of  $\sigma_0$  vs  $f$  in linear units (LU) for each pol-view flavor, for the WVCs of Fig. 2. HH (VV) stands for H-Pol (V-Pol) and F (A) stands for fore (aft). Solid lines: regression curves for each pol-view flavor. The color code is identical. Fig. 4: scatter-plot of  $\sigma_0$  vs  $f$  in LU after correction, for each pol-view flavor (same WVCs of Fig. 3). Color code and acronyms are the same as in Fig. 3. Note that upper y-axis extreme is 10+ times lower than in Fig. 3.

## Conclusions

- The correction scheme is effective to reduce  $\sigma_0$  contamination from land
- Coastal sampling gain: 400%+ ( $\approx 300\%$ ) within 5 (10) km to the coast
- Bias vs ECMWF increases. The reasons are not easily discernable
- Encouraging consistency with SAR-derived winds
- Noise regularization may under-correct within 10 km to the coastline

## Future work

- MLE threshold tuning
- Validate winds (how? Buoys? SAR-derived winds? Consistency checks?)
- Export noise regularization to other pencil-beams scats (OceanSat, HY-2)
- In parallel, improve SAR-derived winds with ResNet method

## Bibliography

- M. P. Owen and D. G. Long, "Land-contamination compensation for quikscat near-coastal wind retrieval," IEEE Transactions on Geoscience and Remote Sensing, vol. 47, no. 3, pp. 839–850, 2009.
- J. Vogelzang and A. Stoffelen, "Ascat land correction, report for the eumetsat ocean and sea ice saf," tech. rep., Koninklijk Nederlands Meteorologisch Instituut, 2022. SAF/OSI/CDOP3/KNMI/TEC/TN/584.
- Fore, A.G.; Süles, B.W.; Strub, P.T.; West, R.D. QuikSCAT Climatological Data Record: Land Contamination Flagging and Correction. Remote Sens. 2022, 14, 2487. <https://doi.org/10.3390/rs14102487>
- Grieco, G.; Stoffelen, A.; Verhoef, A.; Vogelzang, J.; Portabella, M. Analysis of Data-Derived SeaWinds Normalized Radar Cross-Section Noise. Remote Sens. 2022, 14, 5444. <https://doi.org/10.3390/rs14215444>
- Zanchetta and Zecchetto, "Wind direction retrieval from Sentinel-1 SAR images using ResNet", Remote Sensing of Environment, 253, 2021 (<https://doi.org/10.1016/j.rse.2020.112178>).
- G. Grieco, M. Portabella, J. Vogelzang, V. A., and S. A., "Initial development of pencil-beam scatterometer coastal processing", tech. Rep., Barcelona Expert Center (BEC ICM-CSIC), 2020. OSI-SAF VS Technical Report # OSI-SAF 20-01.
- G. Grieco, M. Portabella, J. Vogelzang, V. A., and S. A., "QuikSCAT normalized radar cross section noise characterization for coastal wind field retrieval", tech. Rep., Barcelona Expert Center (BEC ICM-CSIC), 2020. OSI-SAF VS Technical Report # OSI-SAF 20-03.
- G. Grieco, M. Portabella, A. Stoffelen, J. Vogelzang and A. Verhoef, "Towards Quikscat-Derived Coastal Winds," 2021 IEEE International Geoscience and Remote Sensing Symposium IGARSS, 2021, pp. 7307-7310, doi: 10.1109/IGARSS47720.2021.955494

## $\sigma_0$ correction

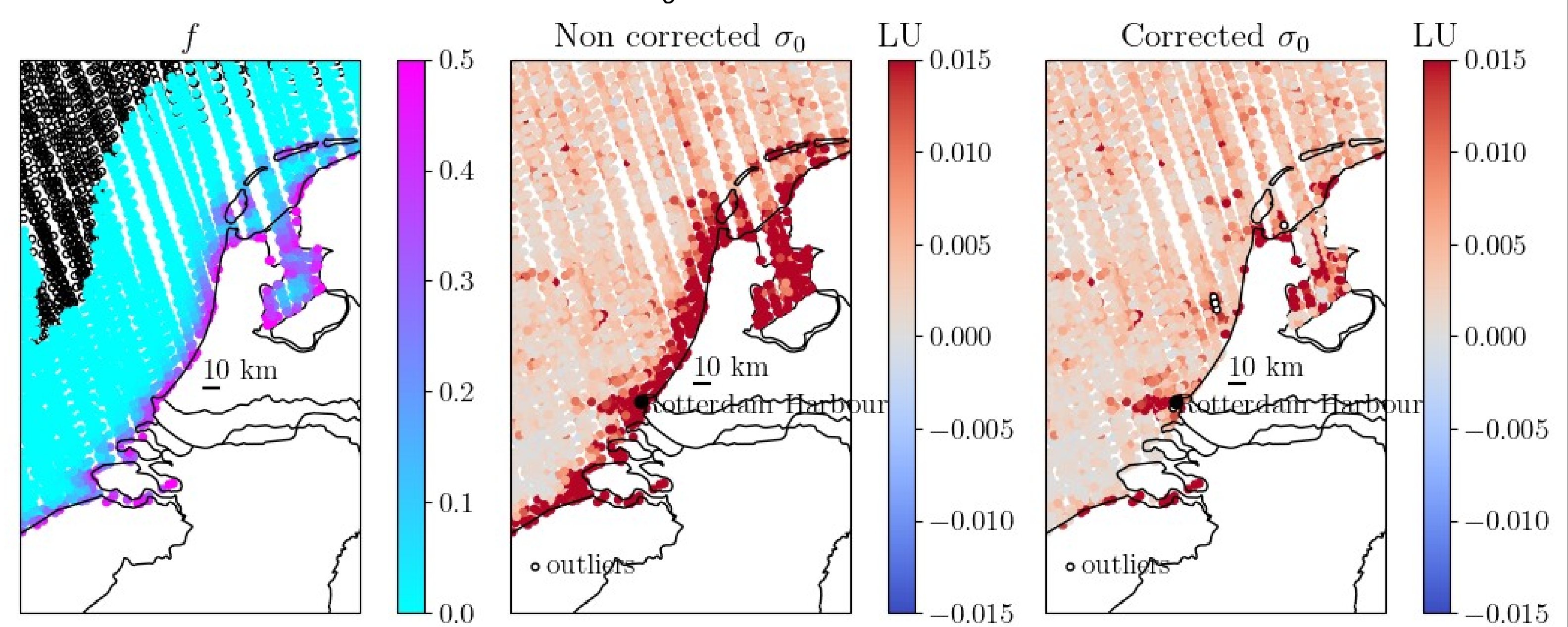


Fig. 3:  $f$  offshore Netherlands. Empty circles:  $f = 0$ . Fig. 4:  $\sigma_0$  before correction. Fig. 5:  $\sigma_0$  after correction. Failures (outliers) are reported as empty circles.

## Ocean Vector Wind (OVW) retrieval @ 12.5 km

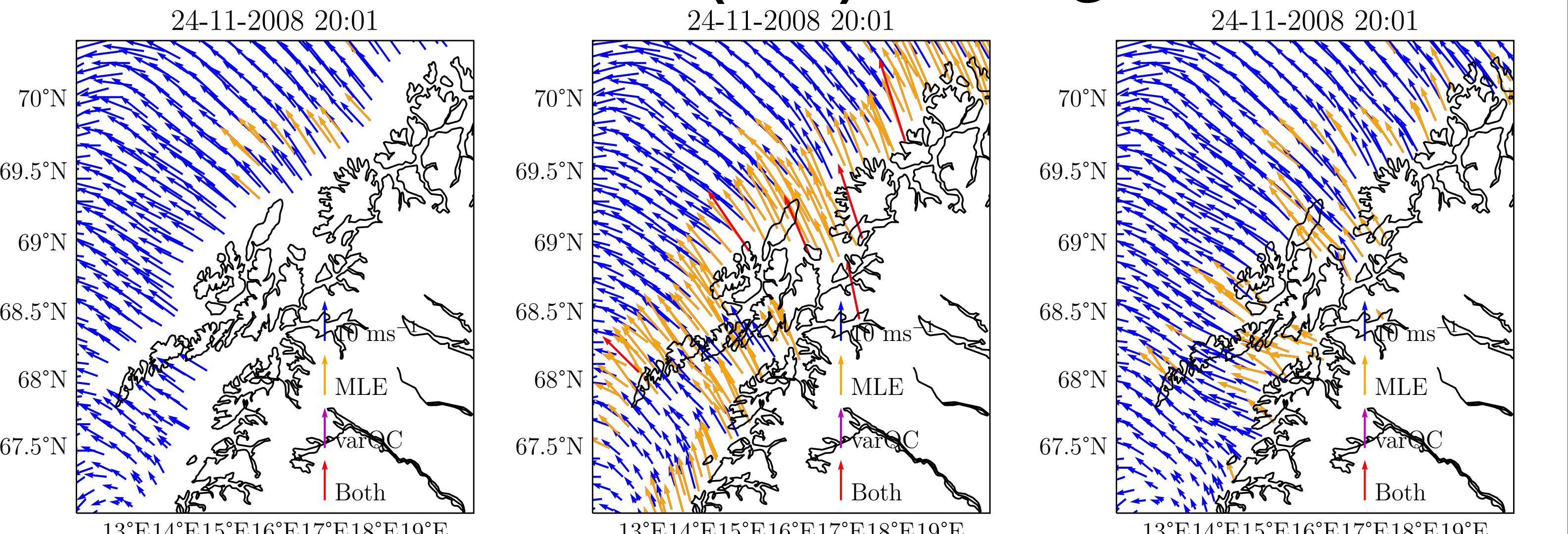


Fig. 6: OVWs offshore Norway.  $\sigma_0$ s with  $f > 0.02$  are discarded. No  $\sigma_0$  correction is applied. Fig. 7: OVWs offshore Norway.  $\sigma_0$ s with  $f > 0.5$  are discarded. No  $\sigma_0$  correction is applied. Fig. 8: OVWs offshore Norway.  $\sigma_0$ s with  $f > 0.5$  are discarded.  $\sigma_0$  correction is applied.

## Comparison to SAR-derived winds (work in progress)

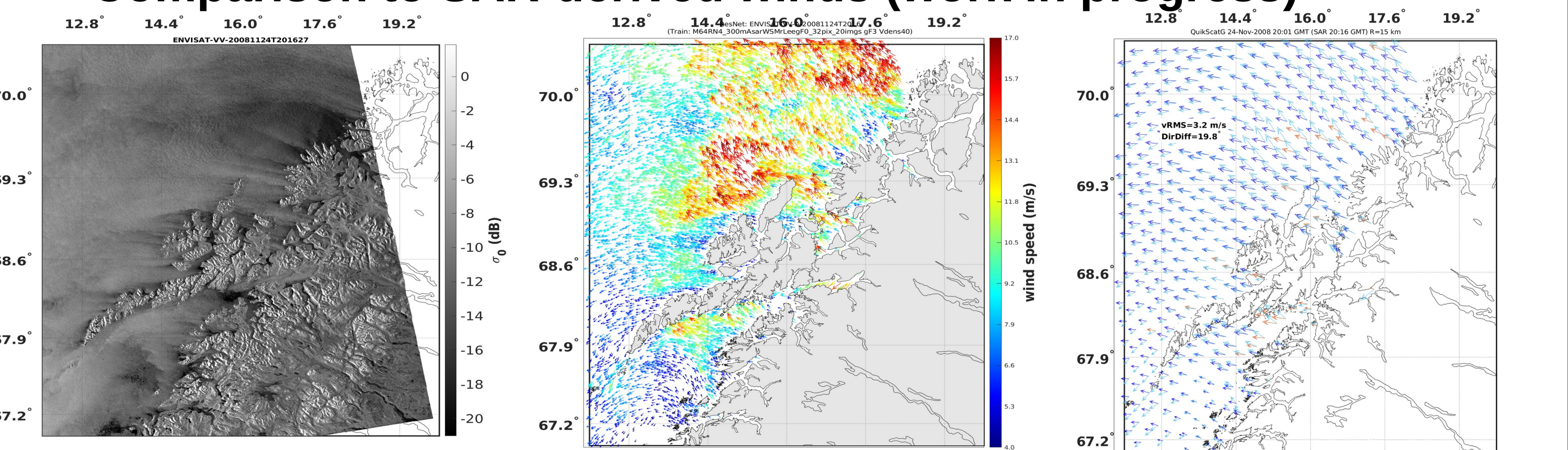


Fig. 9: Left: ASAR  $\sigma_0$  offshore Norway. Center: SAR-derived winds with ResNet [5]. Right: QuikScat (SAR)-derived OVWs in blue (light blue). Rainy winds are in orange. SAR-derived winds are averaged on a circle of 15 km radius around QuikSCAT WVC centroids.

## Sampling gain

## Wind speed pdfs & Comparison to ECMWF

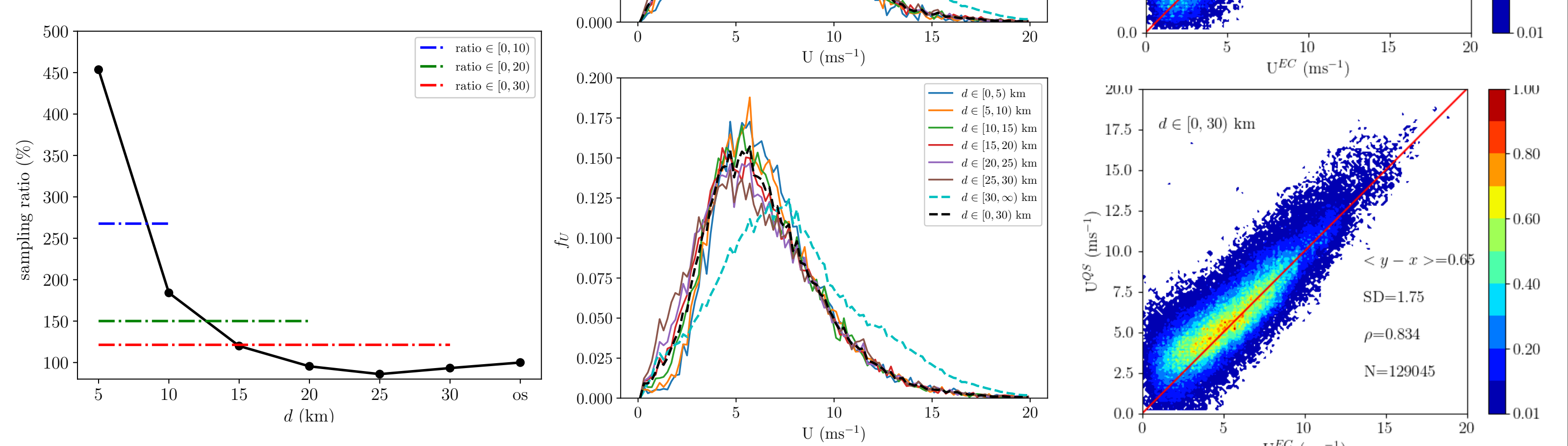


Fig. 10: Top (Bottom): pdfs of wind speed segregated according to distance before (after)  $\sigma_0$  correction is applied.  $\sigma_0$  with  $f > 0.5$  ( $f > 0.5$ ) are discarded. Fig. 11: Top (Bottom): 2D histogram of QuikSCAT-derived vs ECMWF wind speeds before (after)  $\sigma_0$  correction is applied.  $\sigma_0$  with  $f > 0.02$  ( $f > 0.5$ ) are discarded.

## Acknowledgements

- EUMETSAT OSISAF projects OSI\_VSA\_20\_01, OSI\_VSA\_20\_03, OSI\_VSA\_21\_03, OSI\_VSA\_22\_02
- Special thanks to Prof. Dave Long from the BYU and Drs Roy Scott Dumber and Brian Styles from JPL